McMillin-Wood, J., Bush, B., Pitts, B. J. R., & Schwartz, A. (1977) *Biochem. Biophys. Res. Commun. 74*, 677-684.
Morel, F., Lauquin, G., Lunardi, J., Duszynski, J., & Vignais, P. V. (1974) *FEBS Lett. 39*, 133-138.
Murray, W. J., Reed, K. W., & Roche, E. B. (1980) *J. Theor. Biol. 82*, 559-572.
Pande, S. V. (1975) *Proc. Natl. Acad. Sci. U.S.A. 72*, 883-887.
Pande, S. V., & Blanchaer, M. C. (1971) *J. Biol. Chem. 246*, 402-411.
Pande, S. V., & Parvin, R. (1980) in *Carnitine Biosynthesis, Metabolism and Functions* (Frenkel, R. A., & McGarry, J. D., Eds.) pp 143-157, Academic Press, New York.
Patel, K. M., Sklar, L. A., Currie, R., Pownall, H. J., Morrisett, J. D., & Sparrow, J. T. (1979) *Lipids 14*, 816-818.
Powell, G. L., & Churchich, J. E. (1978) *Biochem. Biophys. Res. Commun. 85*, 927-933.
Pullman, M. E. (1973) *Anal. Biochem. 54*, 188-198.
Ramsay, R. R., & Tubbs, P. K. (1975) *FEBS Lett. 54*, 21-25.
Roseman, M. A., & Thompson, T. E. (1980) *Biochemistry 19*, 439-444.
Solberg, H. E. (1974) *Biochim. Biophys. Acta 360*, 101-112.
Wolkowicz, P. E., & McMillin-Wood, J. (1980) *J. Biol. Chem. 255*, 10348-10353.
Yalkowsky, S. H., & Zografi, G. (1970) *J. Pharm. Sci. 59*, 798-802.
Ziegler, H. J., Brackner, P., & Binon, F. (1967) *J. Am. Chem. Soc. 32*, 3989-3991.

Polymerization of the Tubulin–Colchicine Complex and Guanosine 5′-Triphosphate Hydrolysis†

Danièle Saltarelli and Dominique Pantaloni*

ABSTRACT: The tubulin–colchicine (1:1) complex was shown to be able to polymerize in vitro under the buffer conditions of microtubule assembly from pure native tubulin. The physical characteristics of this peculiar polymer have been investigated under a variety of conditions and compared with those of microtubules. Polymerization consisted of a nucleation followed by a growth process, was characterized by a critical concentration, and exhibited divalent ion, temperature, and pH dependences very similar to those of microtubules. Guanosine 5′-triphosphate (GTP) or 5′-guanylyl methylenediphosphate (GMPPCP) was required for polymerization, and guanosine 5′-diphosphate (GDP) was a potent inhibitor. GTP hydrolysis was totally disconnected from the polymerization process and occurred as well under nonpolymerizing conditions. The results are discussed in view of the different types of protein–protein interactions exhibited by tubulin and of the possible relationship between the conformation of the GTP site and the interaction areas.

Substoichiometric amounts of colchicine are known to inhibit the microtubule assembly process in vivo as well as in vitro (Taylor, 1965; Olmsted & Borisy, 1973; Wilson et al., 1975). Colchicine binds to tubulin with a high affinity (Bryan, 1972; McClure & Paulson, 1977), and the quasi-irreversible binding permits the isolation of the tubulin–colchicine complex and its use as an excellent tool in the investigation of the mechanism of assembly via inhibition studies. In this respect, the following points have been established: Two types of tubulin–tubulin interactions are involved in the microtubule wall, namely, strong longitudinal interactions along protofilaments and weaker lateral interactions (Erickson, 1974; Amos & Baker, 1979; Erickson & Pantaloni, 1981). While colchicine does not bind to tubulin once incorporated in the microtubule (Wilson & Meza, 1973), except to the ends (Margolis & Wilson, 1977), the colchicine site is still accessible on linear polymers such as rings (Weisenberg & Timasheff, 1970; Penningroth, 1980) in which only longitudinal interactions between tubulin molecules are involved. Recently Sternlicht & Ringel (1979) reported the possibility of a very slight incorporation of tubulin–colchicine in the microtubule; this copolymerization would then be made possible pending a destabilization of the microtubules in proportion with the amount of tubulin–colchicine incorporated. All these data suggested that the colchicine site is close to one of the two lateral interaction areas of tubulin (David-Pfeuty et al., 1979). Furthermore, the findings that a GTPase activity is induced on tubulin by colchicine binding (David-Pfeuty et al., 1979) and that GTP[1] is hydrolyzed on microtubules in a first-order process subsequent to tubulin assembly (Carlier & Pantaloni, 1978) are suggestive of a connection between the conformation of one of the two lateral interaction areas and the behavior of the GTP exchangeable site, which is located on the β subunit (Geahlen & Haley, 1979). In this hypothesis, both the GTP site and the colchicine site, which genetic studies indicate to be also located on the β subunit (Cabral et al., 1981; Sheir-Neiss et al., 1978), would be in a close vicinity to the lateral interaction area of the β subunit, which seems bound to an α subunit of the adjacent protofilament by a loose protein bridge observable on electron micrographs (Amos & Klug, 1974; Erickson, 1974).

† From the Laboratoire d'Enzymologie, Centre National de la Recherche Scientifique, 91190 Gif-sur-Yvette, France. *Received June 9, 1981; revised manuscript received October 23, 1981.* This work was supported by the Centre National de la Recherche Scientifique, Délégation Générale à la Recherche Scientifique et Technique, the Institut National de la Santé et de la Recherche Médicale, and La Ligue Nationale Francaise Contre le Cancer. A former report of these results has been presented at the 2nd International Symposium on Microtubules and Microtubule Inhibitors at Beerse (Belgium), Aug 1980.

[1] Abbreviations: GTP, guanosine 5′-triphosphate; GDP, guanosine 5′-diphosphate; Mes, 2-(*N*-morpholino)ethanesulfonic acid; EGTA, ethylene glycol bis(β-aminoethyl ether)-*N*,*N*,*N*′,*N*′-tetraacetic acid; EDTA, ethylenediaminetetraacetic acid; ATP, adenosine 5′-triphosphate; DEAE, diethylaminoethyl; NTP, unspecified nucleoside 5′-triphosphate; GMPPCP, 5′-guanylyl methylenediphosphate.

0006-2960/82/0421-2996$01.25/0

The possibility of interactions between molecules of tubulin–colchicine has been investigated with the view of getting a deeper insight into the nature of the tubulin–tubulin interactions and their relation to the events at the exchangeable nucleotide site. The experiments reported here show that the tubulin–colchicine complex is able to self-assemble into non-microtubular polymers under medium conditions identical with those under which unliganded tubulin assembles in microtubules. These polymers are observable in electron microscopy, and their formation can be monitored turbidimetrically. Their physicochemical properties are very similar to those of microtubules and have been investigated: their formation requires a critical concentration, a pH close to neutrality, a temperature above 30 °C, and the presence of GTP and divalent cations. In contrast with microtubules, GTP hydrolysis occurs independently of assembly.

Materials and Methods

Tubulin Purification. Tubulin was purified from pig brain by three cycles of assembly–disassembly according to Shelanski et al. (1973), followed by phosphocellulose chromatography according to Weingarten et al. (1975), in order to remove the microtubule-associated proteins. The obtained solution was concentrated up to 5–10 mg/mL by filtration in an Amicon concentration cell equipped with a PM30 Diaflo membrane and stored at −60 °C in 50 mM Mes, pH 6.6, buffer containing 0.25 mM $MgCl_2$, 0.5 mM EGTA, and 3.4 M glycerol. This solution was used within 2 weeks without any appreciable loss in its ability to polymerize or to bind colchicine.

Protein Assay. Tubulin concentration was determined by the method of Lowry et al. (1951) with the correction of 11% excess coloration as compared with the bovine serum albumin standard (David-Pfeuty et al., 1977).

Colchicine Binding Assay. Colchicine binding to tubulin was determined according to the method of Sherline et al. (1974). Tubulin at a concentration of 10–50 μM was incubated at 37 °C for 30 min with an excess of [^{3}H]colchicine (Amersham). The unbound colchicine was then adsorbed on activated charcoal (3 mg/mL). The supernatant of the centrifuged suspension was assayed for protein concentration and radioactivity. The extent of colchicine binding was usually 0.8–1.0 [^{3}H]colchicine/molecule of tubulin dimer.

GTP Hydrolysis Measurement. The liberation of [^{32}P]P_i occurring upon hydrolysis of [γ-^{32}P]GTP was measured according to Nishizuka et al. (1968). The samples were preincubated at 4 °C for 20 min, a period during which no GTP was hydrolyzed. The reaction was started by a temperature jump from 4 to 37 °C. Aliquots of 50 μL were removed at different times of the reaction and mixed with 450 μL of a 0.25 N $HClO_4$ solution. A 1-mL aliquot of a 0.600 mM KH_2PO_4 solution and 0.5 mL of a 4 N H_2SO_4 solution containing 5% ammonium molybdate were added. The phosphomolybdate complex was extracted with 2 mL of 2-methyl-1-propanol–cyclohexane (1:1 v/v). A 1-mL aliquot of the organic phase was poured in 10 mL of Aquasol or Bray, and the radioactivity was assayed in a Packard liquid scintillation spectrometer.

Polymerization Measurements. The self-assembly of the tubulin–colchicine complex was monitored by electron microscopy and turbidimetry at 420 nm in a Beckman Acta V spectrophotometer equipped with a thermostated cylindrical cell of 0.3-cm diameter and 0.5-cm light path, coupled to a T-jump apparatus that ensured a temperature raising time of 15 s. Unless otherwise indicated, assembly was assayed under standard conditions at 37 °C in the "polymerization buffer" consisting of 50 mM Mes, pH 6.6, containing 1 mM GTP, 10 mM $MgCl_2$, 3.4 M glycerol, and 0.5 mM EGTA.

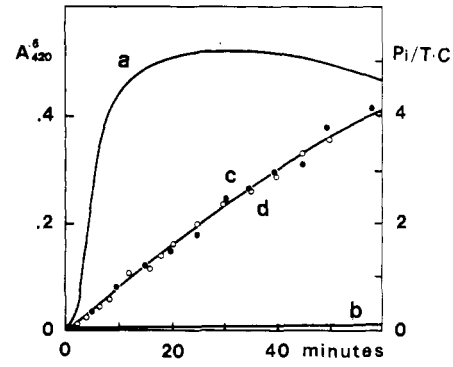

FIGURE 1: Time courses of tubulin–colchicine polymerization and GTP and GTP hydrolysis. Tubulin–colchicine at a concentration of 19 μM was polymerized at 37 °C in the polymerization buffer containing 115 μM GTP (see Materials and Methods). (a and b) Turbidimetric recording at 420 nm of the polymerization process. (c and d) GTP hydrolysis measurements. (a and c) (●) = 10 mM Mg^{2+} ions; (b and d) (○) = 0.25 mM Mg^{2+} ions.

The polymers formed at 37 °C were sedimented at 160000*g* for 5 min in a Beckman airfuge. The air driven through the centrifuge was warmed by passing through a heated bath in order to avoid cooling of the rotor during the centrifugation. The weight concentration of polymer was derived from the difference between the total concentration of protein and the protein concentration of the supernatant. It was checked that the latter did not decrease with longer centrifugations, which indicated that the sedimentation coefficient of the polymer was at least 100 S.

Analytical Ultracentrifugation Measurements. Ultracentrifugation studies were performed in a Beckman Model E instrument equipped with an electronic speed control and a RTIC temperature control unit. The runs were done in 12-mm, 20-sector Kel-F cells. Sedimentation coefficients were obtained from the displacement of the peak of the schlieren pattern. A planimeter was used in the peak area measurements.

Electron Microscopy Studies. Samples were negatively stained with 2% uranyl acetate without fixation and observed in a Hitachi HU 11B electron microscope.

Results

When a solution of the tubulin–colchicine complex at a concentration of 2 mg/mL in polymerization buffer was brought to 37 °C, an increase in turbidity developed following a lag phase (Figure 1). The whole kinetic phenomenon was very similar to the formation of microtubules from pure tubulin in the same medium (Carlier & Pantaloni, 1978).

The assembly of tubulin–colchicine was cold reversible and required a minimal Mg^{2+} ion concentration, like the formation of microtubules from pure tubulin. However, this type of assembly differs from microtubule assembly by an essential feature: Electron microscopy reveals the presence of a large number of polydisperse amorphous aggregates having an average size of 0.3 μm. These aggregates seem to result from the irregular association of coiled structures (Figure 2). Better resolved images showing evidence for whorled double filaments of tubulin–colchicine have previously been presented (Kirschner & Williams, 1974; Matsumura & Hayashi, 1976; Wiche et al., 1979; Sandoval & Weber, 1979). Figure 2b shows that in the presence of GDP, pure tubulin–colchicine (in the absence of MAPs) assembles in double rings, which eventually transform, at high tubulin concentration, into paracrystals, similar to the crystals of rings of pure unliganded tubulin described by Erickson (1974) and R. H. Crepeau, K.

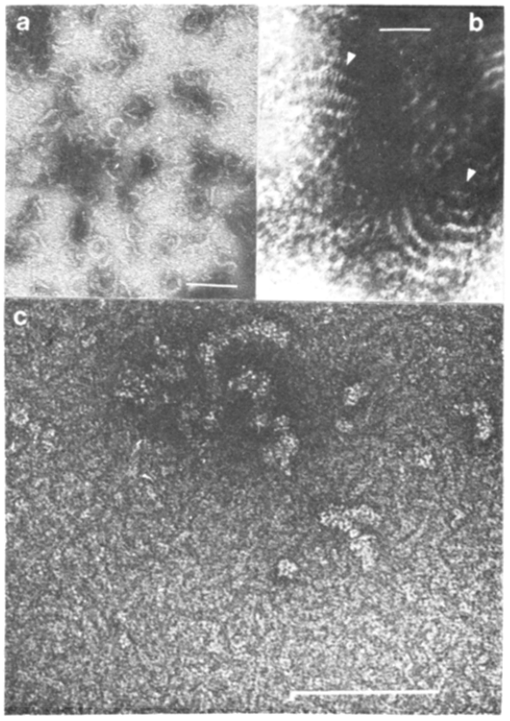

FIGURE 2: Electron micrographs of tubulin–colchicine polymer (bar = 0.1 μm). In the presence of GDP, tubulin–colchicine assembles into concentric double rings (a) that stack at high concentration (8 mg/mL) and form paracrystals (b). Arrows point to a front view and a side view of stacking rings. Ring diameter is 390 Å and the stacking interval is 84 Å. In the presence of GTP (c), no more rings are present. Curved filaments of larger curvature than rings are observed with a repeating motif of 42 Å; they are often laterally associated together, leading to aggregates, a small fragment of which is shown in (c).

E. Fram, D. Pantaloni, and S. J. Edelstein (unpublished results).

Catalytic GTP hydrolysis is another property of the tubulin–colchicine complex; this GTPase activity is not affected by polymerization and is independent of the Mg^{2+} concentration between 0.25 and 10 mM, a range in which a large variation is exhibited in the rate and extent of polymerization. Essential qualitative observations are summarized in Figure 1. The role of different physicochemical parameters in the assembly process will now be studied in detail.

Polymerization Studies at Different Concentrations of the Tubulin–Colchicine Complex. Figure 3 shows that the self-assembly of the tubulin–colchicine complex is characterized by the existence of a critical concentration of 1 mg/mL, below which no polymer can be formed. Under the same conditions the critical concentration for the assembly of tubulin in microtubules was 0.3 mg/mL. Above the critical concentration, the weight concentration of polymer increased linearly with tubulin–colchicine concentration with a rate of 1. The increase in turbidity at 420 nm upon polymerization was proportional to the increase in the concentration of polymer in solution, obtained from sedimentation measurements, with a rate θ_{420} = 1.1 cm^{-1} mg^{-1} mL. When ΔA^1_{420} was higher than 1.6, the relation between the absorbance and the polymer concentration was no longer linear, and a correction involving a viriel coefficient was necessary. The specific turbidity measured for microtubules in the same medium at the same wavelength was θ_{420} = 0.35 cm^{-1} mg^{-1} mL.

Double logarithmic plots of the turbidity reached at equilibrium vs. the wavelength λ were linear and exhibited a negative slope of 2, in contrast with the usual value of 4 characteristic of small molecules and 3 found for microtubules (Gaskin et al., 1974). This result indicated that the three

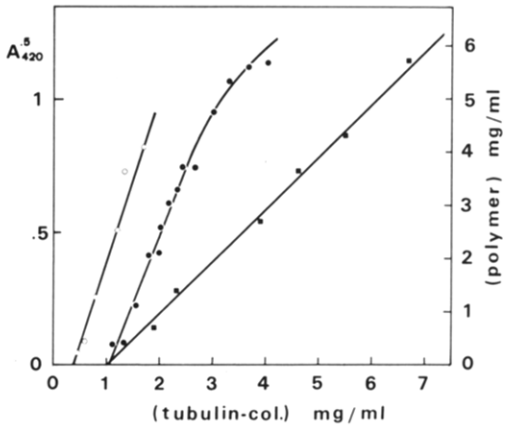

FIGURE 3: Extent of tubulin–colchicine polymerization vs. total tubulin–colchicine concentration, under standard conditions as described under Materials and Methods. (●) Turbidity measurements at 420 nm; (■) weight number of polymer formed determined by sedimentation; (○) turbidity measurements when Mg^{2+} was replaced by 8 mM Ca^{2+}.

dimensions of the polymer were not small as compared to the wavelength. The polymers in solution could be directly observed in dark-field or phase-contrast optical microscopy as well as by epifluorescence due to the presence of bound colchicine. They appeared roughly globular in the optical microscope and were approximately 0.3 μm in diameter.

The time course of polymerization was monitored turbidimetrically. A linear relationship between the observed turbidity and the weight concentration of polymer is verified as soon as the size of the polymer is not too small as compared to the wavelength. In the present case, the polymer average diameter is about 0.1 μm (=λ/4) when its weight concentration is 10% of the equilibrium value. Therefore, at least the last 90% of the turbidity time courses can be analyzed in terms of weight concentration of polymer. The whole polymerization process consisted in two phases. A lag time preceded the development of turbidity according to a pseudo-first-order process. The existence of a lag time and of a critical concentration was indicative of a spontaneously nucleated polymerization. The pseudo-first-order increase in turbidity that developed after the lag time was attributed to the growth process as in the case of microtubules, and the same equation describing the growth of polymers from a constant number of nuclei M fitted adequately to the data:

$$-\mathrm{d}C(t)/\mathrm{d}t = k_+M[C(t) - C_c]$$

where $C(t)$ is the concentration of the monomer tubulin–colchicine at time t, C_c the critical concentration reached at equilibrium, k_+ the elongation rate constant, and M the concentration of nuclei. The observed first-order growth rate constant is $k_{obsd} = k_+M$.

As in the case of helicoidal polymerization (Oosawa & Higashi, 1967) or two-dimensional and three-dimensional polymerization, it can be demonstrated (Erickson & Pantaloni, 1981) that the critical concentration for a large polymer is equal, within a close approximation, to the reciprocal of the dissociation constant K_p for the equilibrium between the polymer and free subunits.

The data presented in Figure 4 are obtained by an analysis of the time courses of polymerization at different concentrations of tubulin–colchicine and show that the lag time corresponding to the nucleation process decreases when the concentration of tubulin–colchicine complex increases. The slope n of the plot log $1/\tau$ vs. log $[C(t) - C_c]$ was 6 ● 0.5. This value is related to the number $2n - 1$ of successive reaction

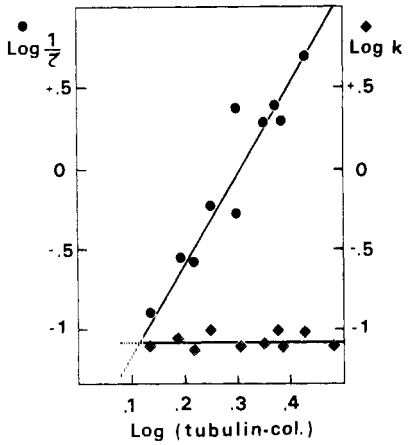

FIGURE 4: Cooperativity involved in the kinetics of tubulin–colchicine polymerization under standard conditions. $1/\tau$ is the reciprocal of the lag time preceding polymer formation and k_1 is the pseudo-first-order rate constant observed for the growth process, in min^{-1}.

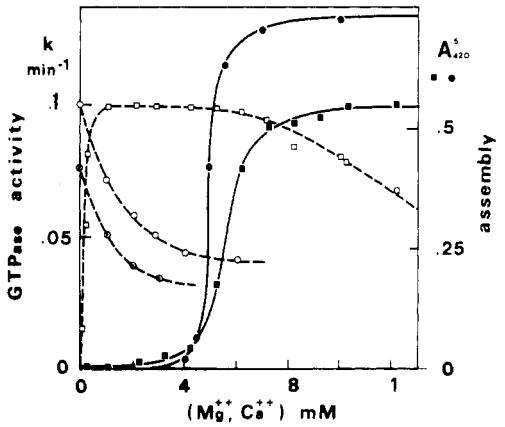

FIGURE 5: Effect of Mg^{2+} and Ca^{2+} ions on the polymerization and GTPase activity of tubulin–colchicine. Tubulin–colchicine concentration was 2.3 mg/mL. (Solid lines) Polymerization measurements under otherwise standard conditions. (Dashed lines) GTP hydrolysis measurements under the same conditions except GTP concentration was 115 μM. (□ and ■) Mg^{2+} ion concentration was varied; (○ and ●) Ca^{2+} ion concentration was varied. The specific turbidities of Ca^{2+} and Mg^{2+} polymers are actually identical, and the critical concentrations are different. Inhibition of the GTPase activity by Ca^{2+} was measured in the presence of 0.25 (○) and 1 mM (⊙) Mg^{2+} ions.

steps that are necessary to form a nucleus of $2n$ molecules (Oosawa & Higashi, 1967). The size of this nucleus (12 tubulin–colchicine molecules at 35 °C) was the same as that found for the formation of microtubules from pure tubulin in identical medium conditions (Carlier & Pantaloni, 1978). The rate constant measured for the growth process was independent of the concentration of the tubulin–colchicine complex and has a value of 0.3 min^{-1} at 37 °C.

Role of Mg^{2+} and Ca^{2+} Ions in Polymerization. The self-assembly of tubulin–colchicine at 37 °C in the presence of GTP was dependent on the concentration of divalent cations Mg^{2+} or Ca^{2+} (Figure 5). The lag period preceding the formation of large polymers was a decreasing function of Mg^{2+} ion concentration (data not shown). The measured degree of cooperativity in the dependence of the lag time on Mg^{2+} ion concentration was 2.4. On the other hand, the first-order rate constant measured for the growth process was independent of Mg^{2+} ion concentration.

At equilibrium the amount of polymer formed, as measured by turbidimetry or sedimentation, was found to increase very cooperatively with Mg^{2+} or Ca^{2+} concentration (Figure 5). The critical concentration was 0.5 mg/mL in the presence of Ca^{2+} and 1 mg/mL in the presence of Mg^{2+}. As clearly

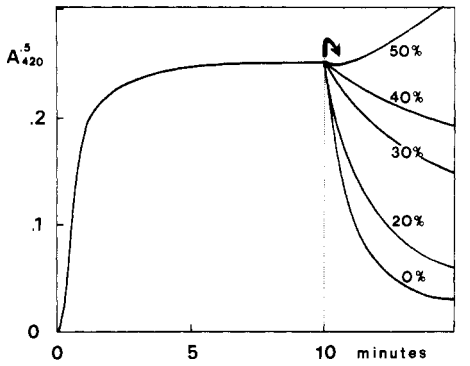

FIGURE 6: Effect of glycerol on polymerization at 37 °C and depolymerization at 4 °C under otherwise standard conditions. Concentrations of glycerol (in percent v/v) were varied as indicated. The solution was cooled to 4 °C at the time indicated by the arrow. Tubulin–colchicine concentration was 1.6 mg/mL.

pointed out by Lee & Timasheff (1977), the theory of linked functions (Tanford, 1961; Wyman, 1964; Pantaloni, 1965) predicts that when an ion or a ligand is involved in a conformation change or a change in the state of the polymerization, the equilibrium is displaced toward the species for which its affinity is the highest and the following equation is valid:

$$\partial \log K / \partial \log a_X = \Delta\bar{\nu}$$

where K in the present case represents the elongation equilibrium constant, a_X is the activity of the ligand X, and $\Delta\bar{\nu}$ is, within a close approximation, the number of ligand molecules apparently involved in the conformation or polymerization change. The total concentration of Mg^{2+} or Ca^{2+} can be likened to its activity, in the 3–10 mM range, since this is 3 orders of magnitude higher than the tubulin concentration and since the amount of GTP–Mg complex (GTP_{total} = 100 μM) can be neglected. Then the slope of the linear plot of log K vs. log [Mg^{2+}] or log [Ca^{2+}] gives a value of $\Delta\bar{\nu}$ of 6 for Mg^{2+} and 20 for Ca^{2+}. The concentrations of divalent cations necessary to obtain the half-extent of polymerization were about 5 mM for either Ca^{2+} or Mg^{2+}.

These polymers readily dissociate below 30 °C at all concentrations of Mg^{2+} or Ca^{2+}, but at very high concentrations (>10 mM) the irreversible formation of aggregates takes place.

Role of Glycerol in Polymerization. While microtubule assembly was greatly promoted by glycerol, the rate and extent of tubulin–colchicine polymerization were totally unaffected by glycerol up to 8 M (Figure 6). However, the cold sensitivity of the polymer formed in the presence of glycerol was affected: dissociation at 0 °C took place more and more slowly as the glycerol concentration was increased, and even a significant turbidity increase was observed at 50% glycerol. These results may indicate that the formation of another type of aggregate, from the polymer formed at 37 °C, occurs at the same time as the depolymerization of tubulin–colchicine polymers and this obscures the turbidity decrease.

Effect of Temperature. The temperature dependence of the three following characteristic properties of tubulin–colchicine was studied: GTP hydrolysis, rate of polymerization, and equilibrium of polymerization. In the investigated concentration range (>2.2 mg/mL) the GTPase activity of tubulin–colchicine was detectable above 17 °C, while its ability to polymerize appeared above 30 °C. Figure 7 shows that when temperature increases from 30 to 40 °C, the lag time preceding polymerization decreases and the polymerization rate constant as well as the amount of polymer increases. The assembly equilibrium at each temperature is characterized by

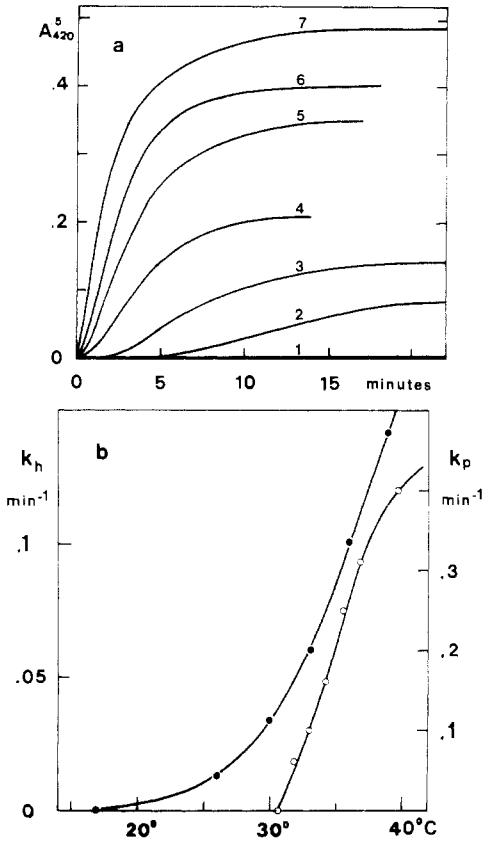

FIGURE 7: (a) Effect of temperature on the lag time and on the rate and extent of polymerization of tubulin–colchicine under otherwise standard conditions. Temperatures were (from curve 1 to curve 7) 30.7, 31.8, 32.7, 34.2, 35.8, 36.8, and 39.7 °C. Tubulin–colchicine concentration was 2 mg/mL. (b) Temperature dependence of the equilibrium and kinetic parameters of polymerization and GTPase activity of tubulin–colchicine. (○) Plot of the evolution of the pseudo-first-order growth rate constant. (●) Plot of the catalytic rate constant of the GTPase activity.

Table I: Thermodynamic Parameters of Tubulin-Colchicine Polymer Growth[a]

T (°C)	ΔC_c (mg/mL)	$\ln K_{app}$	ΔH°_{app} (kcal/mol)	ΔS°_{app} (eu)
31.8	1.76	−10.97		
32.7	1.65	−11.06	18.6	83
34.2	1.45	−11.18	15.0	71
35.3	1.12	−11.40		
36.8	0.90	−11.50	12.7	64
39.7	0.85	−11.60	6.68	−12

[a] $\Delta C_{p_{app}} = -1600 \pm 300$ cal/(mol deg).

the equilibrium association constant $K_c = C_{critical}^{-1}$.

As in the case of microtubules studied by Lee & Timasheff (1977), a pronounced curvature (not shown) was observed in the van't Hoff plot from which the values of the free energy ΔG°, enthalpy ΔH°, and entropy ΔS° changes in the assembly reaction as well as the change in heat capacity ΔC_p could be calculated. The data are summarized in Table I and can interestingly be compared with the corresponding values obtained by Lee & Timasheff (1977) for the formation of microtubules. In particular, the same apparent change in heat capacity, $\Delta C_p = -1600$ cal/(mol deg), and the same positive change in enthalpy and entropy as for microtubule formation were found. A slight difference appeared, however, in the values of the thermodynamic parameters that were identical with those obtained for microtubules at a 6 °C lower temperature. These results lead to the conclusion reached by Lee & Timasheff concerning the loss of ordered water involved in the formation of each tubulin–tubulin contact.

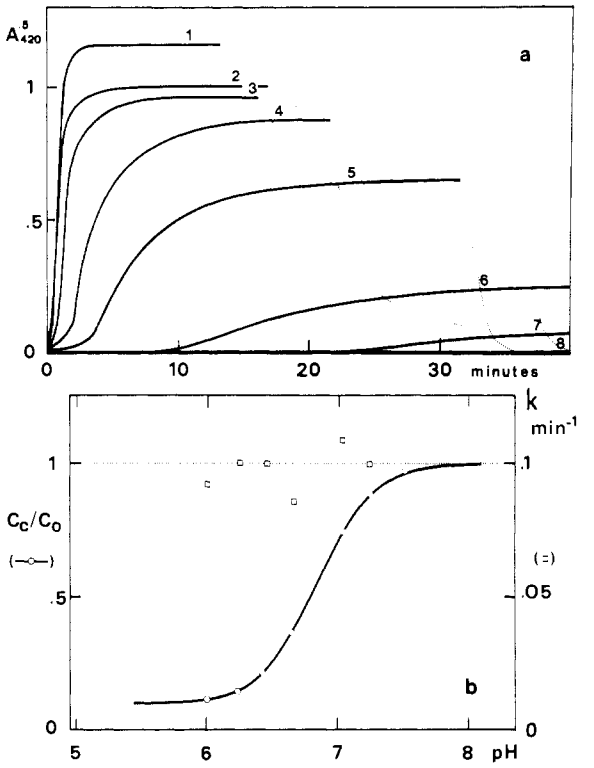

FIGURE 8: Effect of pH on tubulin–colchicine polymerization. (a) Recordings of the evolution of turbidity with time under standard conditions at the following pHs (top to bottom): 5.68, 6.00, 6.23, 6.42, 6.63, 7.06, 7.25, and 7.55. Tubulin–colchicine concentration was 2.9 mg/mL. (b) (○) Plot of the critical concentration C_c normalized with respect to the total concentration C_0 vs. pH. The data are those of (a). The solid curve is the best fitting to the equation $C_c/C_0 = [1 + 10^{n(pK'-pH)}]/[1 + 10^{n(pK-pH)}]$ obtained for the following values of the parameters: $n = 2$, $pK = 6.4$, and $pK' = 6.9$. (□) Plot of the pH dependence of the GTPase activity (k_a).

Table II: Kinetic and Thermodynamic Parameters of the Rate of Growth of Tubulin–Colchicine Polymer[a]

T (°C)	k_p (10^{-3} s^{-1})	$\ln k_p$	$\Delta G^{\circ\ddagger}$ (kcal/mol)	$\Delta H^{\circ\ddagger}$ (kcal/mol)	$\Delta S^{\circ\ddagger}$ (eu)
31.8	1.06	−6.85	21.8		
32.7	1.65	−6.41	21.5	91.1	369
34.2	2.67	−5.93	21.2	60.1	265
35.5	4.17	−5.48	21.0	65.6	145
36.8	5.17	−5.27	20.8	28.7	25
39.7	6.67	−5.01	20.7	17.4	10

[a] $\Delta C_{p_{app}} = -12\,000 \pm 2000$ cal/(mol deg).

Kinetic data for the assembly of tubulin–colchicine at different temperatures are presented in Figure 8 and in Table II. The Arrhenius plot (not shown) deviated strongly from linearity. Eyring's theory of transition states was used to determine the characteristics of the activated complex involved in the assembly reaction. The association rate constant k_a is expressed by

$$k_a = (kT/h)K_c^\ddagger$$

where $K_c^\ddagger$ is the equilibrium dissociation constant of the intermediary activated complex, k the Boltzmann constant, h the Planck constant, and T the absolute temperature. The free energy change accompanying the formation of the activated complex is

$$\Delta G^{\circ\ddagger} = -RT \log K_c^\ddagger = \Delta H^{\circ\ddagger} - T\Delta S^{\circ\ddagger}$$

where $\Delta H^{\circ\ddagger}$ and $\Delta S^{\circ\ddagger}$ are the activation enthalpy and entropy, respectively.

A large value was found for the activation enthalpy, e.g., 90 kcal mol^{-1} at 32 °C. The reaction was made possible through a very large positive entropy change of +369 eu which could indicate that a large number of water molecules are liberated in the association process.

The strong temperature dependence of the thermodynamic parameters seems to point to a complex mechanism consisting of a sequence of reactions of different kinds, e.g., an exothermic process following an endothermic one, as suggested by Hinz et al. (1979) and Berkowitz et al. (1980) for microtubule formation. In such a case, increasing temperature can speed up the rate-limiting endothermic process until the exothermic reaction, which is slowed down in the same time, becomes itself rate limiting at high temperature. A similar phenomenon has already been observed and analyzed (Pantaloni, 1965) in the case of β-lactoglobulin, whose temperature-dependent self-aggregation is inhibited at high temperature. Consequently the measured thermodynamic parameters do not refer to the same kinetic process at all temperatures. In the present case, in the overall change with temperature of the observed constant k_+M are involved the temperature dependences of both the elongation rate constant k_+ and the rate constants of the n successive kinetic processes building up the nucleus. The resulting complexity may cause the observed deviation from linearity in the Arrhenius plots.

Effect of pH on Tubulin–Colchicine Self-Assembly. Tubulin–colchicine self-assembly occurs in a narrow pH range, as has previously been observed for microtubule assembly (Gaskin et al., 1974; Regula et al., 1981). The effect of pH on assembly and disassembly was complex; however, Figure 8a shows that both the rate and extent of assembly increased with decreasing pH in the pH 7.5–5.5 range. The rate and extent of disassembly upon cooling were affected as well. Around pH 7 assembly proceeded to a low extent and was preceded by a long lag time. The optimum pH for reversible assembly was around pH 6, where both the rate and extent of polymerization were high. Below pH 6 the extent of assembly increased up to almost 100% material polymerized, but polymerization was no more reversible upon cooling, showing that a different type of tubulin–tubulin interactions took place at this pH, which is close to the isoelectrical point. A similar behavior has been observed by Gaskin et al. (1974) in the case of native tubulin assembly in microtubules.

The pH dependence of the ratio C_c/C_0 (where C_0 and C_c are the total tubulin and critical concentrations, respectively) has been studied in the pH range 6–7.5 in which polymerization was cold reversible (Figure 8b).

This parameter is highly dependent on pH. The sigmoidal shape of the representation of C_c/C_0 in a narrow pH range is more suggestive of the specific involvement of some particular ionizable groups in the association rather than of a nonlocalized electrostatic effect due to a change in the net charge of the protein. The following reaction scheme can be proposed to account for the data (the predominant species are in boxes):

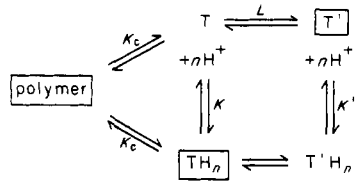

In this model, tubulin is assumed to exist in two states T and T′ in equilibrium. Only the T species would be able to polymerize. Both T and T′ can be protonized. The equilibrium constant L between T and T′ therefore depends on the activity of H^+ ions in the medium. According to Tanford (1961), "if a protein molecule can exist in the conformations α and β, and if the equilibrium constant β/α depends on pH, then a necessary consequence of the laws of thermodynamics is that at least one titrable group has a different pK in the two conformations". Consequently

$$\begin{aligned} pK &= \log [TH]/[T] + pH \\ pK' &= \log [T'H]/[T'] + pH \end{aligned} \tag{1}$$

A change in pH will cause a shift in the equilibrium between T and T′, the equilibrium constant varying between the two limit values $L = [T']/[T]$ and $L\alpha = [T'H]/[TH]$, where $\alpha = 10^{pK'-pK}$. The change in pH results in a change in the apparent critical concentration, defined as

$$C_c^{app} = [T] + [TH] + [T'] + [T'H] \tag{2}$$

Since within this model the equilibrium association constant for the polymer formation, defined as

$$K_c = 1/([T] + [TH]) \tag{3}$$

remains constant when the pH is changed, the polymerizable fraction of soluble tubulin can be written as

$$\bar{X}_t = ([T] + [TH])/([T] + [TH] + [T'] + [T'H]) \tag{4}$$

Comparison of eq 2–4 shows that

$$C_c^{app} = (K_c\bar{X}_t)^{-1}$$

and

$$\bar{X}_t = \left(1 + L\frac{1 + 10^{pK'-pH}}{1 + 10^{pK-pH}}\right)^{-1} \tag{5}$$

In the general case where n protons are cooperatively involved in the conformational change T $\rightleftharpoons$ T′, the following equations can be written:

$$\begin{aligned} npK &= \log [TH]/[T] + npH \\ npK'' &= \log [T'H]/[T'] + npH \end{aligned} \tag{6}$$

which leads to the general expression of the apparent critical concentration:

$$C_c^{app} = K_c^{-1}\bar{X}_t^{-1} = K_c^{-1}\left[1 + L\frac{1 + 10^{n(pK'-pH)}}{1 + 10^{n(pK-pH)}}\right] \tag{7}$$

When pH increases, C_c^{app} varies between the two limit values $K_c^{-1}(1 + \alpha^n L)$ and $K_c^{-1}(1 + L)$.

The ratio between the values of the critical concentration before and after the transition is

$$(1 + \alpha^n L)/(1 + L) \tag{8}$$

and can be obtained experimentally. A value of 10 was determined for this ratio from the data shown on Figure 8. Obviously $L = [T']/[T] \gg 1$ and therefore α^n can be approximated to 10. The parameters of eq 7 were determined by fitting the experimental plot to the theoretical curve, and a satisfactory adjustment was obtained with the values n = 2, pK = 6.4, and pK' = 6.9. Two protons thus appear to be simultaneously involved in a conformation change of tubulin–colchicine, which permits a modulation of its ability to polymerize in a narrow pH region close to neutrality.

The experimental data presented are not sufficient yet to allow the determination of the nature of the ionizable groups involved in these linked functions: they could be either two homologous groups in the dimer tubulin, imidazole, lysine, carboxylate, etc. or a ionizable group in a ligand bound to tubulin such as GTP whose pK in the free state is 6.5 or a

molecule of morpholinoethanesulfonic acid whose pK in the free state is around 6.

GTPase Activity of the Tubulin–Colchicine Complex. The GTPase activity induced by colchicine binding to tubulin has first been reported in this laboratory (David-Pfeuty et al., 1979). Total and stoichiometric inhibition of this activity by vinblastine has eliminated the possibility of a GTPase contaminating the tubulin preparation. The present study shows that this activity requires magnesium ions with an apparent $K_m(Mg^{2+})$ of 50 μM at 37 °C. Figure 1 emphasizes the different magnesium dependences of polymerization and GTP hydrolysis. GTP hydrolysis was inhibited by EDTA and by an excess of magnesium ions with an inhibition dissociation constant $K_I(Mg^{2+})$ of 15 mM. Ca^{2+} ions also inhibited GTP hydrolysis to a maximum of 60%. The inhibition was of the noncompetitive type toward Mg^{2+}, and the same value of 1.2 mM was determined for the Ca^{2+} inhibition equilibrium constant in the presence of 0.25 and 1 mM Mg^{2+}.

GTP hydrolysis was unaffected by up to 30% glycerol (v/v) under the following conditions: 24.5 μM tubulin–colchicine, 0.2 mM GTP, 10 mM Mg^{2+}, and 2.5, 5, 15, 19, 22, 26, and 30% glycerol. The measured turnover rate constant was 0.092 $\pm$ 0.006 min^{-1}. This result is in contrast with those obtained for microtubule assembly dependent GTP hydrolysis, which is affected by glycerol in a manner parallel to the ability of tubulin to polymerize. GTP hydrolysis was unaffected by a change in pH in the range studied (pH 6–7.5) (Figure 8b).

The very low turnover rate of GTP hydrolysis on tubulin colchicine necessitates, to be accurately measurable, the presence in the enzymatic assays of unusually high enzyme concentrations, i.e., in the 10^{-5} M range. Under such conditions where the concentrations of substrate and enzyme are of the same order of magnitude, the accurate determination of the Michaelis constant K_m of GTP is not possible from the usual Lineweaver–Burk plot. However, estimation of the K_m(GTP) was attempted, taking into account the amount P_i of GTP hydrolyzed during the first 3 min of the reaction (the first time interval assayed), the amount of GTP bound to tubulin, and the inhibition due to GDP produced ([GDP] = [P_i]), by using a value of 65 μM for the inhibition dissociation constant K_I, determined in a separate experiment. A corrected estimation of the free substrate (S) concentration was calculated from the total concentrations of tubulin (T_0) and of added GTP (S_0) according to

$$[S] = [S_0] - [P_i] - [T_0]v/V_{max}$$

A plot of $1/v$ vs. $1/[S]$ yielded an apparent value K_m^{app} for GTP. The intrinsic value was determined from

$$K_m = K_m^{app}/(1 + [P_i]/K_I)$$

A value of 10 μM was thus determined for the Michaelis dissociation constant of GTP for tubulin–colchicine. Since the Mg^{2+} concentration was 1 mM in these experiments and since the equilibrium dissociation constant of the GTP–Mg chelate is in the 10^{-5} M range, almost all the GTP is in the form GTP–Mg, which then is likely to be the substrate of the GTPase reaction.

The rate of GTP hydrolysis was strongly temperature dependent (Figure 7b). The thermodynamic data given in Table III can be compared with those of Table II that characterize polymerization, showing no simple correlation between GTP hydrolysis and tubulin–colchicine polymerization. Again high values were found for the activation entropy and enthalpy. The question to be dealt with is whether the activated complex responsible for GTP hydrolysis results from an intramolecular structural change of the tubulin molecule similar to the conformational change induced by colchicine binding reported by Garland (1978).

Table III: Kinetic and Thermodynamic Parameters of GTP Hydrolysis by the Tubulin–Colchicine Complex

T (°C)	k_h (10^{-4} s^{-1})	ln k_h	$\Delta G^{\ddagger}$ (kcal/mol)	$\Delta H^{\ddagger}$ (kcal/mol)	$\Delta S^{\ddagger}$ (eu)
17	0.13	−11.25	23.7		
26	2.3	−8.38	21.7	54.7	112
30	5.7	−7.47	21.5	80.0	195
33	10.0	−6.91	21.1	68.0	156
36	16.7	−6.39	20.8	64.0	142
39	23.7	−6.04	20.7	22.4	7.7

All the above listed features characterizing the GTPase activity of the tubulin–colchicine complex demonstrate the absence of a close connection between polymerization and GTP hydrolysis. In this respect the behavior of the tubulin–colchicine complex is different from that of unliganded tubulin.

Role of Nucleotides in Tubulin–Colchicine Polymerization and GTPase Activity. Preliminary experiments showed that tubulin–colchicine polymerized as well in the presence of GMPPCP, a nonhydrolyzable analogue of GTP, which gives further evidence for the complete disconnection between assembly and nucleotide hydrolysis. On the other hand, GDP was inefficient in promoting polymerization or in stabilizing the polymer, contrary to the case of microtubules in the same medium (Carlier & Pantaloni, 1978; Zackroff et al., 1980). ATP was inefficient as well, provided there was complete removal of the NDP kinase activity by chromatography of tubulin on DEAE-cellulose (Jacobs & Huitorel, 1979). Without this precaution, GTP can be regenerated from ATP and GDP bound to tubulin, and polymerization can take place as in the case of microtubule formation.

A thorough investigation of polymerization as a function of GTP concentration is hampered by GTP hydrolysis on tubulin–colchicine. Indeed, at GTP concentrations lower than 100 μM, no equilibrium polymerization plateau could be reached. Figure 9a shows the turbidity curves recorded at a series of GTP concentrations. The initial increase in turbidity was immediately followed by a spontaneous depolymerization, which occurred sooner when the GTP concentration was lower. This observation indicates that polymerization and GTP hydrolysis must be studied simultaneously and the GTP and GDP concentrations must be determined at each time. The fact that the amount of polymer formed and the rate of GTP hydrolysis both decrease as GDP accumulates in the medium and that the rate of GTP hydrolysis is unaffected by polymerization can be accounted for by a simple model in which tubulin–colchicine would hydrolyze GTP at the same rate in either the dimer or polymer form and in which tubulin–colchicine–GDP would not polymerize and would be merely a poorly represented transient species in the polymer.

Within this model, the rate v of GTP hydrolysis and the amount [P] of polymer at equilibrium are described by

$$v = V_M([P] + [T\text{–}GTP])/C_0 \quad (9)$$

$$[P] = C_0 - ([T\text{–}GTP] + [T\text{–}GDP] + [T]) \quad (10)$$

in which C_0, [P], and ([T–GTP] + [T–GDP] + [T]) represent the weight concentrations of total, polymerized, and free tubulin–colchicine, respectively.

Equation 9 can be written as

$$[P] = (v/V_M)C_0 - [T\text{–}GTP] \quad (11)$$

Since only the GTP-bound tubulin–colchicine species participates in the polymerization process, T–GTP concentration

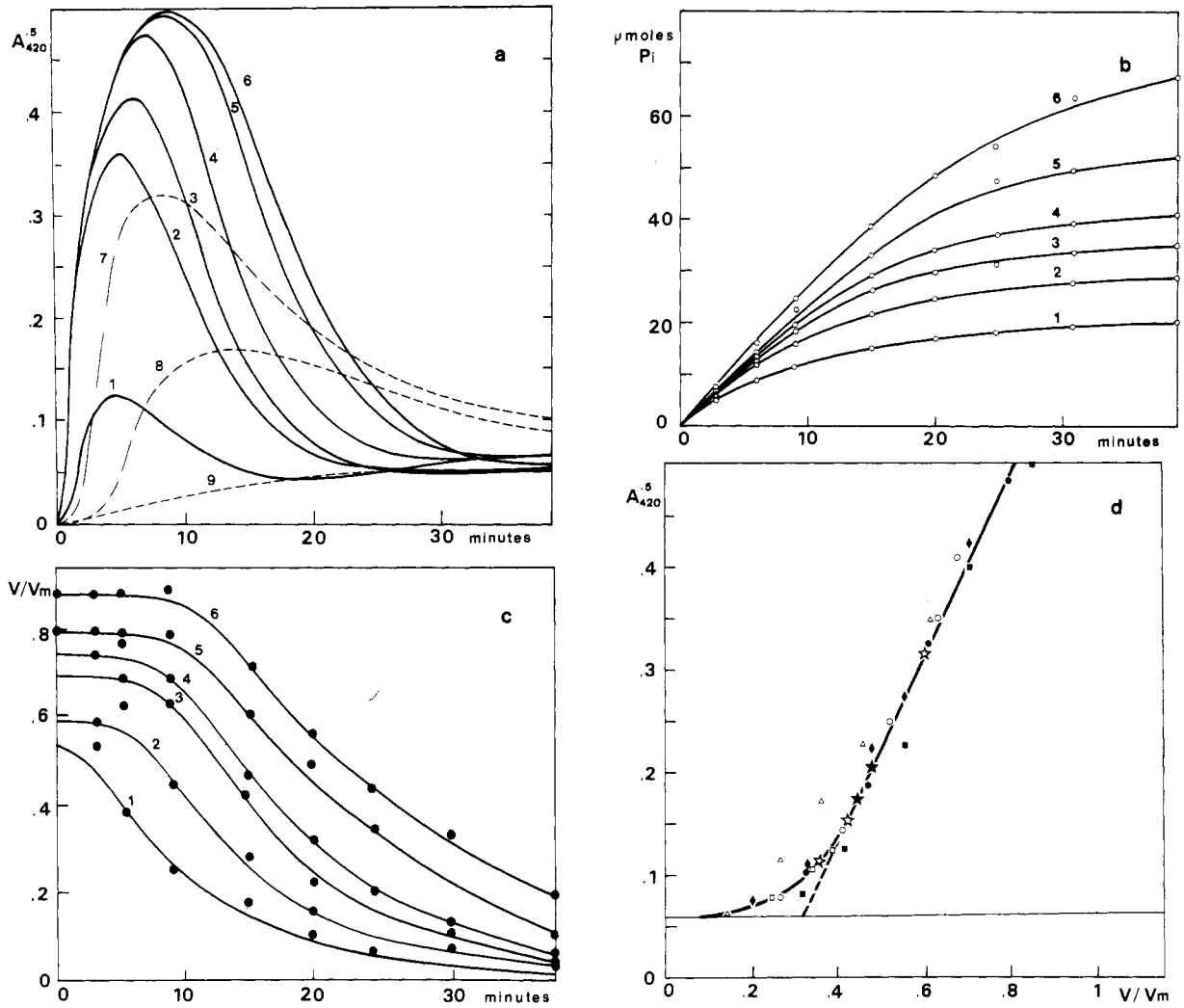

FIGURE 9: Correlation between the balance GTP/GDP, the amount of polymer, and the rate of GTP hydrolysis. (a) Evolution with time of the amount of polymer at different initial concentrations of GTP: curves 1–6 = 30, 40, 50, 60, 80, and 100 μM. Tubulin–colchicine concentration was 2.4 mg/mL. Otherwise standard conditions. (b) Simultaneous measurement of liberated P_i in the same experiment. Curves 1–6 refer to the same assays as in (a). (c) Evolution of the rate of GTP hydrolysis with time. Data from Figure 9b have been derived with respect to time and normalized with respect to the extrapolated initial maximal rate V_M. (d) Linear relation between the depolymerization steps shown in (a) and the corresponding decrease in the rate of GTP hydrolysis shown in (c). The following symbols refer to the corresponding numbered curves: (△) 2; (○) 3; (♦) 4; (●) 5; (■) 6; (☆) 7; (★) 8. (Dashed curves) Inhibition by GDP of polymerization and GTPase activity of tubulin–colchicine. Time course of the polymerization reaction under standard conditions except GTP concentration was 50 μM and GDP was added at zero time at the following concentrations: curves 3, 7, 8, and 9 = 0, 50, 200, and 300 μM, respectively. Simultaneous measurement of the time course of P_i liberation was performed (data not shown).

is the intrinsic critical concentration C_c for the formation of the polymer.

Taking into acount the equilibrium dissociation constants for nucleotides binding to tubulin–colchicine, eq 9 and 10 are transformed into

$$\frac{v}{V_M} = 1 + \left(\frac{C_c}{C_0} \frac{K_{GTP}}{[GTP]} + \frac{K_{GTP}}{K_{GDP}} + \frac{[GDP]}{[GTP]} \right) \quad (12)$$

$$P = C_0 - C_c \left(1 + \frac{K_{GTP}}{[GTP]} + \frac{K_{GTP}}{K_{GDP}} \frac{[GDP]}{[GTP]} \right) \quad (13)$$

As GDP accumulates due to GTP hydrolysis, the T–GDP complex is formed to the detriment of the polymer, and as long as polymer exists in solution, the critical concentration C_c of the T–GTP species is maintained. Equation 11 accounts for the relation that necessarily exists between the rate of GTP hydrolysis and the amount of polymer, due to the fact that both parameters are affected by the relative concentrations of GTP and GDP. In support to this view, no spontaneous depolymerization occurred when the polymer was formed in the presence of Ca^{2+}, conditions under which GTP hydrolysis is greatly inhibited.

So that this model could be further tested the values of the turbidity ($A_{420}^{0.5} = 0.5\theta_{420}[P]$) read at different times of the depolymerization process were plotted vs. the relative rates of hydrolysis (v/V_M) measured at the same times. Figure 9d shows that the plots obtained for the series of curves done at different GTP concentrations all lined up on the same straight line as predicted by eq 11. However, in the low absorbance range a slight deviation from the expected turbidity values was observed due to the formation of rings of tubulin–colchicine–GDP as shown in Figure 2. Nevertheless, the data seem to well support the model proposed and emphasize that the depolymerization observed is not a kinetic process but is a consequence of the evolution with time of the ratio [GDP]/[GTP] (eq 13).

When GDP was added before polymerization, the lag time increased considerably. At a tubulin–colchicine concentration of 2.1 mg/mL, in the presence of 50 μM GTP, the lag time was 0.6 min and increased up to 4 min when 200 μM GDP was added. The same lag time would have been obtained if

tubulin–colchicine at a concentration of 1.5 mg/mL had been polymerized in the absence of GDP (Figure 4). If the value of the ratio K_{GDP}/K_{GTP} is assumed to be ~6, the concentrations of T–GTP and T–GDP can be calculated in the presence of 50 μM GTP and 200 μM GDP. A value of 1.44 mg/mL is found for T–GTP, which is very close to 1.5 mg/mL and further corroborates the adequacy of the model within which only the T–GTP species polymerizes.

Discussion

This work demonstrates that the tubulin–colchicine (1:1) complex exhibits a large number of the assembly properties of native tubulin. Since colchicine is known to inhibit microtubule assembly with a high efficiency, the issue started was to examine whether the structural change induced in the tubulin molecule by colchicine binding was important enough to alter all four interaction areas involved in the tubulin–tubulin contacts in the microtubule or whether one area only could be modified. In this respect, only the relative orientation of this area toward its neighbor or the flexibility of the $\alpha\beta$ dimer might be modified.

The results presented demonstrate that tubulin–colchicine can polymerize into nonmicrotubular polymers and that the physicochemical properties of these polymers are very similar to those of microtubules: (1) The assembly is an exponential process, preceded by a lag time. (2) The lag time varies cooperatively with tubulin concentration. The cooperativity number is indicative of the size of the nucleus; its value is $n = 12$ at 35 °C. (3) The assembly is characterized by a critical concentration of tubulin–colchicine under which no polymer can be observed by turbidimetry. (4) Guanosine triphosphate or a nonhydrolyzable analogue (GMPPCP) is required for the formation of the tubulin–colchicine polymer. (5) Guanosine diphosphate is a potent competitive inhibitor of assembly. (6) Divalent cations are necessary for assembly. (7) The pH range in which assembly takes place is pH 6–7. (8) The optimum temperature for assembly is around 30 °C, and a large positive enthalpy and entropy change is involved in the assembly process. The associated change in heat capacity is about −1500 cal/(mol deg). (9) The polymer is cold sensitive. (10) Ring structures and paracrystals can be obtained.

The major differences with microtubules are as follows: (1) The tubulin–colchicine polymer does not exhibit any fibrous structure and appears as an amorphous aggregate of curly filaments in the electron microscope. (2) GTP hydrolysis is not dependent on assembly. (3) GDP does not stabilize the polymer, which therefore has essentially GTP bound. (4) Ca^{2+} ion can replace Mg^{2+} ion in the assembly process but inhibits the GTPase activity. As a result, the GTP polymer should be more stable than in the presence of Mg^{2+}, which may be supported by the lower critical concentration observed. (5) Glycerol does not promote tubulin–colchicine assembly. (6) The critical concentration for the assembly of tubulin–colchicine is higher than for microtubule assembly under the same medium conditions. This higher stability is only 800 cal/mol of tubulin, which is relatively weak and represents only 10% of the total protein–protein interaction energy involved in the microtubule wall. From a global and thermodynamic point of view, colchicine binding does not notably affect the self-assembly properties of tubulin. Only the geometry of the polymer is deeply modified as shown on the electron micrographs (Figure 2). This difference in the polymer morphology may be the consequence of a structural change of the tubulin molecule upon colchicine binding. Indeed, it is well established that colchicine binding is followed by a slight conformation change of the dimer as evidenced by the colchicine fluorescence enhancement (Garland, 1978), the induction of a GTPase activity (David-Pfeuty et al., 1979), the decrease in the equilibrium dissociation constant of the $\alpha\beta$ dimer, and the inability to build up the microtubule lattice. Colchicine binding on the other hand does not affect GTP or vinblastine binding or ring formation.

If we assume, in agreement with Erickson (1974), Kirschner & Williams (1974), and Weisenberg & Timasheff (1970), that the rings represent the coiled species of microtubule protofilaments, it can be inferred that tubulin–tubulin interactions in the rings are of the longitudinal type and positive charge dependent (magnesium ions or MAPs). Therefore, as far as the ability to form ring oligomers is concerned, we can say that the longitudinal interactions are not modified by colchicine binding. In the introduction of this paper we pointed out the established data that were suggestive of colchicine binding to a site located on or in close connection with one of the lateral interaction areas of tubulin.

The thermodynamic stability and specificity of tubulin association and ligand binding reactions result from an original combination of noncovalent interactions, namely, hydrogen bonds, hydrophobic interactions, dispersion (London) forces, and electrostatic interactions. In addition, molecular distortion also may be involved in tubulin association.

At pH 7 the tubulin molecule carries a considerable number of carboxylate groups. A compensation of the resulting repulsive electrostatic interactions by cationic polymers (MAPs, polylysine, DEAE-dextran, etc.) (Erickson & Voter, 1976) or by divalent cations (Mg^{2+}) is needed to promote the formation of curved protofilaments, which are stabilized in the ring structure even at low temperature. A temperature increase leads to microtubule or tubulin–colchicine aggregate formation. Timasheff's results (Lee & Timasheff, 1977) and Table I show that these two aggregating systems are favored by an entropy increase, despite an unfavorable associated enthalpy change. These features must be attributed to the formation of contacts between nonpolar groups, excluding a large number of solvation water molecules. These hydrophobic interactions are unspecific, but salt bridges between unlike charges or hydrogen bonds buried inside the contact domain can contribute fully to the specificity of the lateral interaction between the right side and the left side of protofilaments in the microtubule wall.

It is well-known that microtubule assembly is pH dependent and takes place between pH 6 and pH 8 (Gaskin et al., 1974; Regula et al., 1981). However, when the pH is decreased to below pH 7, erroneous lateral interactions in protofilament assembly can occur and together with microtubules are observed various ribbon-shaped structures, principally "S" and "ω" sheets. These erroneous assembly products arise from a parallel 180° rotation of adjacent protofilaments about an axis parallel to the microtubule axis (Mandelkow & Mandelkow, 1979; D. Pantaloni, B. McEven, and S. Edelstein, unpublished results). Moreover, using the hook appendages as polarity indicators, we have shown that S sheets result from an inversion bringing into contact the left sides of two protofilaments in almost all cases (D. Pantaloni, B. McEven, and S. Edelstein, unpublished results). This erroneous interaction between homologous sides (L–L) of two protofilaments is likely to be the most probable polymerized configuration taken by tubulin molecules that have lost one of their two lateral areas, leading to the formation of double-strand polymers like those formed from tubulin–vinblastine (Himes et al., 1976) and tubulin–colchicine (Matsumura & Hayashi, 1976; Wiche et al., 1979; Sandoval & Weber, 1979).

The heterologous interactions between two hydrophobic areas of the type L–R carrying two unlike charges exhibit a pH dependence in a range complementary to homologous L–L and R–R interactions. More specifically, heterologous interactions could be of the type L–COO^-–^+H_3N–R and homologous interactions L–COOH–HOOC–L and R–NH_2–H_2N–R. Microtubules, in which the L–R interactions are involved, are stable between pH 6.6 and pH 8 (Regula et al., 1981) while aberrant assemblies of microtubules or tubulin–colchicine polymer, in which L–L interactions are involved, appear principally below pH 6.9 and at 37 °C with a cooperativity number of 2. In the case of a model protein, β-lactoglobulin, the existence of one abnormal carboxylate group per subunit has been demonstrated (Tanford, 1961). This group has a pK_a of 7.5 and is titrated with a cooperativity number of 2 due to the formation of a symmetric dimer in which the two promoters are bound through homologous interactions (Pantaloni, 1965). In the case of tubulin, the nature of the ionizable group involved in the formation of the tubulin–colchicine polymer is unknown, but the transition pH of 6.9 suggests the possibility of a carboxylate group that would be protonated concomitantly with the homologous tubulin–tubulin association.

It has been established that the ratio of the longitudinal to lateral bond energies in the microtubule wall is equal to the average ratio of length to width of the sheet usually observed, i.e., ~10 (Carlier & Pantaloni, 1978). The value of the lateral bond energy has been estimated to 1.5–2.3 kcal/mol at 37 °C (Erickson & Pantaloni, 1981). This energy is very weak but can be determinant in the stability and specificity of microtubule assembly. From the data provided by Sternlicht & Ringel (1979), it can be calculated that the destabilization accompanying the incorporation of one molecule of tubulin–colchicine in one microtubule is 27 kcal/mol, while the energy involved in the binding of tubulin–colchicine to a microtubule end is of the same order as for unliganded tubulin, i.e., −7.4 kcal/mol at 37 °C (Lambeir & Engelborghs, 1980). These data can be interpreted within a simple model in which colchicine binding to the lateral area of tubulin β subunit would not notably affect the other interaction areas and consequently permit tubulin–colchicine binding to microtubule ends and to ring oligomers but would considerably hamper the incorporation in the microtubule.

Added in Proof

After this paper was submitted for publication, a manuscript by Andreu and Timasheff was communicated to us, in which evidence was provided for the formation of tubulin–colchicine polymers under conditions similar to ours. However, the polymers described by these authors had a fibrous structure. In contrast, W. A. Voter and H. P. Erickson repeated our experiments and under these conditions checked that "the aggregates are really composed of tubulin rings or coils, closely stacked in somewhat loose and irregular cylinders.... We believe the tubulin–colchicine polymer must be composed entirely of these coils and stacks of rings. These stacks seem to aggregate in an irregular fashion, creating the appearance of an amorphous aggregate".

Acknowledgments

We thank Dr. M. F. Carlier for helpful discussions and her contribution in the redaction of the manuscript. We gratefully acknowledge assistance of Jean Laporte in the electron microscopy experiments.

References

Amos, L. A., & Klug, A. (1974) *J. Cell Sci. 14*, 523–549.

Amos, L. A., & Baker, T. S. (1979) *Nature (London) 179*, 607–612.

Berkowitz, S. A., Velicelebi, G., Sutherland, J. W. H., & Sturtevant, J. M. (1980) *Proc. Natl. Acad. Sci. U.S.A. 77*, 4425–4429.

Bryan, J. (1972) *Biochemistry 11*, 2611–2616.

Cabral, F., Sobel, M. E., & Gottesman, M. M. (1981) *Cell (Cambridge, Mass.) 20*, 29–36.

Carlier, M. F., & Pantaloni, D. (1978) *Biochemistry 17*, 1908–1915.

David-Pfeuty, T., Erickson, H. P., & Pantaloni, D. (1977) *Proc. Natl. Acad. Sci. U.S.A. 74*, 5372–5375.

David-Pfeuty, T., Simon, C., & Pantaloni, D. (1979) *J. Biol. Chem. 254*, 11696–11702.

Erickson, H. P. (1974) *J. Supramol. Struct. 2*, 393–411.

Erickson, H. P., & Voter, W. A. (1976) *Proc. Natl. Acad. Sci. U.S.A. 73*, 2813–2817.

Erickson, H. P., & Pantaloni, D. (1981) *Biophys. J. 34*, 293–309.

Garland, D. (1978) *Biochemistry 17*, 4266–4272.

Gaskin, F., Cantor, C. R., & Shelanski, M. L. (1974) *J. Mol. Biol. 89*, 737–753.

Geahlen, R. L., & Haley, B. E. (1979) *J. Biol. Chem. 254*, 11982–11987.

Himes, R. H., Burton, P. R., & Kersey, P. N. (1976) *Proc. Natl. Acad. Sci. U.S.A. 73*, 4397–4399.

Hinz, H. J., Gorbunoff, M. S., Price, B., & Timasheff, S. N. (1979) *Biochemistry 18*, 3084–3089.

Jacobs, M., & Huitorel, P. (1979) *Eur. J. Biochem. 99*, 613–622.

Kirschner, M. W., & Williams, R. C. (1974) *J. Supramol. Struct. 2*, 412–428.

Lambeir, A., & Engelborghs, Y. (1980) *Eur. J. Biochem. 109*, 619–624.

Lee, J. C., & Timasheff, S. N. (1977) *Biochemistry 16*, 1754–1764.

Lowry, O. H., Rosebrough, N. W., Faur, A. L., & Randall, R. J. (1951) *J. Biol. Chem. 193*, 265–275.

Mandelkow, E. V., & Mandelkow, E. (1979) *J. Mol. Biol. 129*, 135–148.

Margolis, R. L., & Wilson, L. (1977) *Proc. Natl. Acad. Sci. U.S.A. 74*, 3466–3470.

Matsumura, F., & Hayashi, M. (1976) *Biochim. Biophys. Acta 453*, 162–175.

McClure, W. O., & Paulson, J. C. (1977) *Mol. Pharmacol. 113*, 560–575.

Nishizuka, J., Lipman, F., & Lucas Lenarid, J. (1968) *Methods Enzymol. 12*, 713.

Olmsted, J. B., & Borisy, G. G. (1973) *Biochemistry 12*, 4282–4289.

Oosawa, F., & Higashi, S. (1967) *Prog. Theor. Biol. 1*, 79–164.

Pantaloni, D. (1965) Thèse d'Etat, Orsay Série A, no. 128.

Penningroth, S. M. (1980) *Biochem. Biophys. Res. Commun. 92*, 189–190.

Regula, C. S., Pfeiffer, J. R., & Berlin, R. D. (1981) *J. Cell Biol. 89*, 45–53.

Sandoval, T. V., & Weber, K. (1979) *J. Mol. Biol. 134*, 159–172.

Sheir-Neiss, G., Lai, M. H., & Morris, N. B. (1978) *Cell (Cambridge, Mass.) 15*, 639–647.

Shelanski, M. L., Gaskin, F., & Cantor, C. R. (1973) *Proc. Natl. Acad. Sci. U.S.A. 70*, 765–768.

Sherline, P., Bodwin, C. K., & Kipuis, O. M. (1974) *Anal. Biochem. 62*, 400–407.
Sternlicht, H., & Ringel, I. (1979) *J. Biol. Chem. 254*, 10540–10550.
Tanford, C. (1961) *J. Am. Chem. Soc. 83*, 1628–1636.
Taylor, E. W. (1965) *J. Cell Biol. 25*, 145–160.
Weingarten, M. D., Lokwood, A. H., Hwo, S., & Kirschner, M. W. (1975) *Proc. Natl. Acad. Sci. U.S.A. 72*, 1858–1862.
Weisenberg, R., & Timasheff, S. N. (1970) *Biochemistry 9*, 4110–4115.
Wiche, G., Honig, L. S., & Cole, R. D. (1979) *J. Cell Biol. 80*, 553–563.
Wilson, L., & Meza, I. (1973) *J. Cell Biol. 58*, 709–719.
Wilson, L., Anderson, K., Grisham, L., & Chin, D. (1975) in *Microtubules and Microtubule Inhibitors* (Byers, M., & De Brabander, M., Eds.) pp 103–113, American Elsevier, New York.
Wyman, J. (1964) *Adv. Protein Chem. 19*, 224–285.
Zackoff, R. V., Weisenberg, R. C., & Deery, W. S. (1980) *J. Mol. Biol. 139*, 641–677.

Altered Physicochemical Properties of the Deoxyribonucleic Acid–Mitomycin C Complex. Evidence for a Conformational Change in Deoxyribonucleic Acid†

David J. Kaplan‡ and Maria Tomasz*

ABSTRACT: Binding of the antibiotic mitomycin C to sonicated calf thymus DNA results in increased viscosity and an unaltered sedimentation constant of DNA. Flow dichroism measurements of the mitomycin C–DNA complex indicate that the 310-nm absorbance vector of the chromophore of the bound drug is oriented at approximately 57.2° relative to the helix axis. A conclusion drawn from these results is that mitomycin C does not intercalate between base pairs, but rather, it is bound in one of the grooves. Binding of mitomycin C causes a number of changes which are DNA size dependent: (1) increased viscosity of sonicated, decreased viscosity of nonsonicated DNA; (2) unaltered sedimentation rate of sonicated, increased rate of nonsonicated DNA; (3) reduced electrophoretic mobility of nonsonicated DNA; (4) electron microscopic appearance of sonicated DNA–mitomycin complexes which is similar to that of control, while nonsonicated DNA complexes which display highly coiled, looped structures not seen in control nonsonicated DNA. These size-dependent effects are interpreted as indicative of conformational distortion of DNA at rare intervals, caused by a minor fraction of total bound mitomycin. The parallel use of sonicated and nonsonicated DNA as probes for certain effects of drug binding may be useful for detecting this type of phenomenon in general.

Mitomycin C (I) is a potent antibiotic and clinically useful antitumor agent (Remers, 1979). It inhibits cellular DNA synthesis selectively (Shiba et al., 1958) and interacts directly

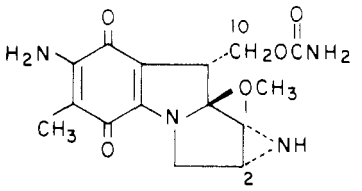

I

with DNA by binding covalently to the individual strands ["monofunctional binding" (Szybalski & Iyer, 1964)], as well as inducing covalent cross-links between the complementary strands (Matsumoto & Lark, 1963; Iyer & Szybalski, 1963). The same types of interaction with DNA can be observed in vitro, but only if a reductive activating agent is added in situ, such as NADPH-dependent bacterial lysates (Iyer & Szybalski, 1964), certain chemical reducing agents (Iyer & Szybalski, 1964; Weissbach & Lisio, 1965), or NADPH-dependent rat liver microsomal preparations (M. Tomasz, unpublished results). These facts indicate that in vivo mitomycin C is converted by reductive metabolism into an active DNA-binding and cross-linking agent (Iyer & Szybalski, 1964). The cross-links were suggested to be the direct cause of the observed inhibition of DNA synthesis and death of bacteria (Iyer & Szybalski, 1963), although the monofunctional binding greatly predominates (10–100-fold) over the cross-links (Szybalski & Iyer, 1964; Weissbach & Lisio, 1965; D. J. Kaplan and M. Tomasz, unpublished results). Indeed, more recently the monofunctional attachment itself has also been implicated as biologically significant damage (Weiss et al., 1968; Kinoshita et al., 1971; Mercado & Tomasz, 1972; Small et al., 1976).

The active form of mitomycin is generated by reduction of the quinone system of I. The reactive, short-lived species has not been isolated or characterized (Iyer & Szybalski, 1964). Covalent interactions with DNA occur in this reduced state (Iyer & Szybalski, 1964; Weissbach & Lisio, 1965), but in the presence of air, the DNA-bound drug is reoxidized to a quinone as seen by the ultraviolet spectral properties of the isolated DNA–mitomycin complexes (Tomasz et al., 1974). The likely structure of the monofunctionally bound drug to DNA is shown in II, as inferred from the ultraviolet spectra, from mitomycin analogue binding studies (Lipman et al., 1978), and from model reactions of mitomycin (Hornemann et al., 1979; Hashimoto et al., 1980; Tomasz & Lipman, 1981). A second alkylating function, assumed because of the observed

† From the Department of Chemistry, Hunter College, City University of New York, New York, New York 10021. *Received October 19, 1981.* This work was supported by a grant from the National Science Foundation (PCM 77-24075) and a CUNY Faculty Research Award.

‡ Present address: College of Pharmacy, University of Kentucky, Lexington, KY 40506.

0006-2960/82/0421-3006$01.25/0